International Journal of Development Mathematics Vol 3 Issue 3, 014–042

INTERNATIONAL JOURNAL OF DEVELOPMENT MATHEMATICS

ISSN: 3026-8656 (Print) | 3026-8699 (Online)

journal homepage: https://ijdm.org.ng/index.php/Journals

Threshold Dynamics and Stability Analysis of a Host-Parasite Model for *Paragonimiasis* with Numerical Simulations

James J. Yakoko[a*], Abdulfatai A. Momoh[b], Musa Samuel[b], Micah Habila[a], and Manju K. Ahmed[c]

[a]Department of Mathematics, College of Education Zing, Taraba State, Nigeria.
[b]Department of Mathematics, Faculty of Physical Science, Modibbo Adama University, Yola, Nigeria.
[c]Department of General Studies Education, Federal College of Education, Yola.

ARTICLE INFO

Article history:

Received 01 May 2026
Received in Revised 28 July 2026
Accepted 08 August 2026

Keywords

Paragonimiasis, Numerical Simulation, Stability Analysis, Threshold Dynamics, Equilibrium states.

MSC 2020 Subject classification: 92D40, 93A30

Abstract

Paragonimiasis, commonly referred to as Lung fluke disease, is a neglected tropical disease that poses a serious risk to public health in endemic areas. Eating uncooked or undercooked freshwater crustaceans that contain *Paragonimus* larvae is the primary way that the disease is spread. This paper develops a system of nonlinear ordinary differential equations that model the interaction between definitive and intermediate host populations with constant control, in order to better understand its transmission. Basic reproduction numbers (R_0) were calculated for the subpopulations in order to assess transmission potential and create essential threshold conditions for disease persistence or extinction. Similarly, under certain conditions, the Castillo-Chavez, Feng, and Huang framework was used to establish the global asymptotic stability of the

*Corresponding author Tel: +2347035007315
Email address: jamesyakoko@coezing.edu.ng;
https://doi.org/10.62054/ijdm/0303.02

DFE. A sensitivity analysis on R_0 was carried out to determine the key variables influencing transmission. The analytical results were supported by numerical simulations, which showed that vaccination and treatment together significantly lower the number of infected classes and can eventually eradicate the disease. Thus, this framework offers important epidemiological insights, showing that increasing vaccination, enhancing treatment and hygiene can successfully lower environmental contamination and manage the spread of *Paragonimiasis* in human population.

1 Introduction

Paragonimiasis a parasitic disease caused by *Paragonimus* species, continues to pose a significant public health threat, particularly in regions where the consumption of raw or undercooked freshwater crustaceans is common. The parasite's transmission cycle, involving multiple hosts humans, snails, cercariae, and crustaceans adds complexity to the disease's epidemiology and complicates effective control measures. Although *Paragonimiasis* exerts substantial health and socio-economic impacts, it remains largely underreported worldwide, with many transmission drivers still poorly understood. As a Neglected Tropical Disease (NTD), *Paragonimiasis* also referred to as lung fluke disease, mostly affects populations in tropical areas (WHO, 2022). The disease has attracted little attention from the international scientific community, especially in the African context, despite recent research showing extensive transmission in Nigeria Iboh (2018); Ibanga (2003). In Nigeria, a comparable pattern emerged. The disease was first recognized as endemic in 1964 but became a public health issue during the Nigerian Civil War (1967–1970). Socioeconomic collapse during the war exacerbated the disease's spread, leading to a high number of cases. However, following the war, a well-organized eradication campaign eliminated *Paragonimiasis* by 1980. No cases were reported from 1980 to September 2007 Enwereji (2010). In October 2007, the disease resurfaced in Nigeria, mimicking the resurgence noted in Japan. This reemergence underscores the challenges of maintaining long-term disease control in resource-limited settings. The reemergence of *Paragonimiasis* in Nigeria poses important public health issue, particularly given its limited awareness and resources for addressing the disease.

When *Paragonimus* miyazakii cases suddenly increased in Japan in 2000, it turned out that people were consuming raw wild boar meat. When praziquantel was administered to patients, they discovered that in roughly 71% to 77% of cases, the infection was resolved after just one day of medication. That increased to 86% to 100% by day two, and they achieved a flawless 100% cure rate by day three. That is quite impressive Nawa (2000). The most important thing to keep in mind is this: It is not advisable to ignore *Paragonimiasis*. It can seriously damage the lungs, resulting in conditions like recurrent *pneumothoraces*, *empyema*, and chronic pleural effusions, if we don't treat it or don't treat it strongly enough. Patients may require VATS, chest drainage, or even lung resections in extreme circumstances. If the parasite enters the brain, it may

cause *eosinophilic meningoencephalitis*, *hydrocephalus*, and visual loss. Although some patients may feel well and remain asymptomatic for years, we shouldn't wait if their serology results are positive. It's not only good practice to give them the regular two- to three-day course of praziquantel; it's crucial to prevent these unpleasant neurological and pulmonary consequences before they arise.

Mathematical modeling has increasingly become an essential tool in investigating the dynamics of infectious diseases, particularly those caused by food-borne trematodes. Yan et al. (2004) outlined the core principles behind the mathematical modeling of food-borne disease transmission and farm-level intervention strategies. Their study highlights how mathematical models can be used to assess the emergence and spread of antimicrobial resistance, especially during antimicrobial treatment in livestock. The use of such medications can leave residual levels in the gastrointestinal tract, fostering the selection and amplification of resistant bacterial strains. By integrating pharmacokinetic (PK) and pharmacodynamics (PD) models with bacterial population dynamics, these models can predict how drug concentrations affect both resistant and susceptible bacterial populations. A flowchart included in their study details a comprehensive model that combines PK/PD modeling with bacterial dynamics accounting for the interactions between susceptible bacteria and those carrying plasmid-borne resistance. Furthermore, the spread of resistance is amplified by bacterial proliferation and horizontal gene transfer, the latter of which can be mathematically modeled as an infectious process Lili et al. (2007). The term used to describe how susceptible bacteria gain plasmids through interaction with resistant bacteria is analogous to the concept of transmission in SIR models $\beta\frac{N_sN_r}{N}$; where β is the conjugation rate represents the frequency at which plasmid transfer occurs, with the variables N_s, N_r and N denoting the populations of sensitive, resistant, and total bacteria, respectively. Most mechanisms of antimicrobial resistance are associated with a fitness cot (α), often reflected as a growth rate (r) in bacteria. This can be modeled by assuming that the growth of resistant bacteria is proportional to that of sensitive bacteria, adjusted by a factor of one minus the fitness cost [r(1-α)]. However, it's important to note that antimicrobial resistance does not always entail a fitness cost Zhang et al. (2006). Yuang et al. (2018) developed a deterministic model for *Clonorchiasis* transmission among human-snail-fish populations, offering critical insights into infection dynamics and intervention strategies. Similarly, Yakoko et al. (2024) made a significant contribution by formulating a mathematical model that captures the transmission mechanisms of *Paragonimiasis* among humans, snails, and crustaceans. Their model effectively employed sensitivity analysis and computational simulations to predict disease prevalence and evaluate the potential impacts of control interventions. The strength of Yakoko et al. (2024) model lies in its clarity, structure, and ability to simulate realistic disease behaviors, laying a strong foundation for future research and policy development. However, despite its insightfulness, the model created by Yakoko et al. (2024) falls short of capturing the complexities of the transmission of *Paragonimiasis* since it leaves out important elements such as vaccinations, symptomatic stages, treatment plans, and optimal control measures. Recognizing this gap, the World Health Organization WHO (2022) stressed the need for integrated approaches to *Paragonimiasis* control, highlighting the roles of vaccination, systematic, treatment and optimal control interventions. Building on this momentum, the present study extends the Yakoko et al. (2024) framework by

incorporating additional disease compartments: vaccinated, symptomatic, and treated human classes, as well as latent and incapacitated stages for snail and crayfish populations. By simulating a more detailed transmission process and applying optimal control strategies, this research seeks to enhance the predictive capacity of Yakoko et al. (2024) models, identify effective intervention strategies and offer practical recommendations for the disease prevention and efforts to curb the disease and its associated socio-economic burden particularly in resource-limited and endemic areas.

2 Formulation of *Paragonimiasis* model

The system was built around five major transmission nodes humans, eggs, snails, cercariae, and crayfish the mathematical model described here effectively represents the intricate lifecycle of *Paragonimiasis*. Each of these populations is further divided into compartments that reflect different stages of parasite development or clinical infection status in order to demonstrate the biological reality of the disease.

1. Human Population Dynamics: The following compartments comprise the human population: Vaccinated humans $V_h(t)$, Susceptible humans $S_h(t)$, Exposed humans $E_h(t)$, Asymptomatically infected humans $I_A(t)$, Symptomatically infected humans $I_S(t)$, Chronically infected humans $I_C(t)$:, Treated humans $T_h(t)$ and Recovered humans with immunity $R_h(t)$. The total number of humans is represented by:

$$N_h(t) = V_h(t) + S_h(t) + E_h(t) + I_A(t) + I_S(t) + I_C(t) + T_h(t) + R_h(t)$$

Vaccinated humans compartment $V_h(t)$ experiences growth due to vaccination at κ rate and decreases due to waning of vaccine at ω rate and μ_h natural death rate. Compartment for susceptible human $S_h(t)$ grow due to recruitment at a steady rate Λ_h, Increase through recovery of treated individuals with permanent immunity at rates ϕ and waning of vaccine at the rate ω due to imperfection of vaccine. Decrease due to infection from consuming improperly cooked crayfish, affected by $\frac{\beta_h S_h I_c}{N_h}$ force of infection is, where β_h represents the rate at which *Paragonimiasis* is transmitted from infected crayfish to humans, accounting for the effect of vaccination administered at a given rate κ, also as a result of natural death at μ_h rate. Exposed Humans compartment $E_h(t)$ increase due to the rate at which susceptible individuals transition to the infected human compartment due to exposure at $\frac{\beta_h S_h I_c}{N_h}$ rate, decrease as individuals progress to the asymptomatic infectious human stage $I_A(t)$ at $rE_h(t)$ rate and as a result of natural mortality occurring at a rate μ_h. Asymptomatic infected human compartment $I_A(t)$ increases as exposed individuals progress at a rate rE_h. Decrease as a result of progression to $T_h(t)$ and $I_S(t)$ at a rate $\psi_1 r_1 I_A$ and $(1-\psi_1)r_1 I_A$ respectively and natural death at μ_h rate. Symptomatic infected human compartment $I_S(t)$ Increase due to progression from asymptomatic infectious human compartment $I_A(t)$ at $(1-\psi_1)r_1 I_A$ rate. Decrease due to progression to treated human compartment $T_h(t)$ and chronically infectious human compartment $I_C(t)$ at $\psi_2 r_2 I_S$ and $(1-\psi_2)r_2 I_S$ rates respectively. Similarly, it also decreases as a result of disease-related mortality and natural death occurring at a rate of d_1 and μ_h. Chronically infectious human compartment $I_C(t)$ Increase due to progression from symptomatic infected human compartment $I_S(t)$ at rate $(1-\psi_2)r_2 I_s$. Decrease due to progression to Treated human compartment

$T_h(t)$ at $\psi_3 r_3 I_C(t)$ rate, declines due to disease-induced mortality at a rate of d_2 and natural death at a rate μ_h.

Treated human compartment $T_h(t)$ Increase due to progression from asymptomatic infected human compartment $I_A(t)$ symptomatic infected human compartment $I_S(t)$ and chronically infected human compartment $I_C(t)$ at a rate $\psi_1 r_1 I_A$, $\psi_2 r_2 I_S$, and $\psi_3 r_3 I_C$, respectively. Decreases due to progression to recovered human compartment $R_h(t)$ at γT_h rate and natural death at μ_h rate. Recovered human compartment $R_h(t)$ Increase due to progression from treated human compartment $T_h(t)$ at γT_h rate, decrease due to progression to susceptible human compartment $S_h(t)$ at ϕ rate and natural death at μ_h rate.

2. Egg Population Dynamics: The egg population $G(t)$ is introduced by infected humans into the environment. Recruitment into $G(t)$ compartments occurred when P_g portion of the eggs is expelled from the infectious host through sputum, feces, or urine, and a portion at rate θ_g successfully enters freshwater, susceptible aquatic snails that come into contact with these eggs become exposed and begin the process of developing cercariae. After an incubation period following the initial contact, the exposed snails transition to the infected state. These infected snails then release a second larval form, known as cercariae, with a fraction P_c being discharged into freshwater at a rate θ_c. When susceptible aquatic snails come into contact with these released eggs, they become exposed to the infection and begin producing cercariae after an incubation period. Once the exposed snails mature, they transition to the infected class and begin releasing a second type of free-swimming larval stage, known as cercariae, at a release rate $\frac{\delta_g \beta_s S_s G}{N_s}$. However, a fraction of the larvae (*miracidium*) is ingested by susceptible snails without causing infection. This indicates that only a fraction of the egg population contributes to the infection dynamics within the snail population.

3. Snail Population Dynamics: The following comprises the snail population: $S_s(t)$ susceptible snail at given time t, $E_s(t)$ exposed snail at given time t, $L_s(t)$ latent snail at given time t, $I_s(t)$ infected snail at given time t and $D_s(t)$ Incapacitate snail at given time t. The total number of snail population is represented by:

$$N_s(t) = S_s(t) + E_s(t) + L_s(t) + I_s(t) + D_s(t)$$

Susceptible snail compartment $S_s(t)$ Growth through the recruitment of individuals into the population at a steady rate Λ_s, reduction is caused by infection through contact with eggs $G(t)$ at $\frac{\beta_s S_s G}{N_s}$ force of infection rate, where β_s is the rate at which eggs are transferred to snails and μ_s natural mortality rate. The exposed snail compartment $E_s(t)$ Increase due to infection from susceptible snail at rate $\frac{\beta_s S_s G}{N_s}$, decrease due to Progress to latent compartment at ε_1 rate and natural death at μ_s. Latent snail compartment $L_s(t)$ Increase due to progression from exposed snail compartment $E_s(t)$ at rate ε_1 decrease due to Progress to the Infected snail compartment $I_s(t)$ at a rate σ and natural death at a rate μ_s. Infected snail compartment $I_s(t)$ Increase due to progression from Latent snail compartment $L_s(t)$ at rate σ, decrease due to Progress to the dead/incapacitated compartment at a rate τ and natural death at μ_s rate. Dead/incapacitated snail compartment $D_s(t)$ Increase due to progression from Infected snail compartment $I_s(t)$ at rate τ and

decrease due to natural death at μ_s rate.

4. Cercariae Dynamics: TThe cercariae population $C(t)$ is released by infected snails: Increase due to release from infected snails at rate $\theta_C P_C I_s(t)$. Decrease as a result of infection of susceptible crayfish, natural decay at $\frac{\delta_c \beta_c S_c C}{N_c}$ rate and natural death at μ_C rate.

5. The crayfish population dynamics are structured across four compartments governed by constant recruitment (Λ_c), predation (p_c), and natural mortality (μ_c). Susceptible crayfish (S_c) enter through recruitment and decrease upon contact with cercariae (C) at force of infection $\frac{\beta_c S_c C}{N_c}$ to join the exposed class (E_c). Exposed individuals transition into latency at rate ε_2, after which latent crayfish progress to the infected compartment (I_c) at rate σ_1. Finally, infected crayfish advance to the dead/incapacitated class (D_c) at rate τ_1, with all classes exiting the system via predation and natural death.The total number of crayfish population is represented by:

$$N_c(t) = S_c(t) + E_c(t) + L_c(t) + I_c(t) + D_c(t)$$

Table 1. *Paragonimiasis* model parameters.

Variable	Description
Λ_h	Recruitment rate into susceptible human compartment
Λ_s	Recruitment rate into susceptible snails compartment
Λ_c	Recruitment rate into susceptible crayfish compartment
β_h	Transmission rate from infected crayfish to humans
β_s	Transmission rate from eggs to snails
β_c	Transmission rate from cercariae to crayfish
ω	Waning rate of vaccine in human
κ	Vaccination rate
μ_h	Death rate of human
μ_s	Death rate of snail
$\mu_c + p$	Death rate and predation rate of crayfish
μ_g	Death rate of meta cercariae eggs
μ_C	Death rate of cercariae
P_c	Number of cercariae in every infected snail
P_g	Number of embryonated eggs passed by each infected human
θ_g	Rate of eggs in fresh water
θ_c	Rate of cercariae released from infected snails
d_1	Disease induced death in symptomatically infection
d_2	Disease induced death in chronically infection
r	Progression rate from exposed to asymptomatic infectious human

Table 1: *Paragonimiasis* model parameters Cont.

Variable	Description
r_1	Rate of progression to symptomatic infected individual
r_2	Rate of progression from symptomatic to recovered
r_3	Rate of progression from chronic to recovered
δ_c	Per consumption rate of the eggs by crayfish
δ_g	Per consumption rate of the eggs by snail
ε_1	Proportion of snails in latent that become infectious
ε_2	Proportion of crayfish in latent that become infectious
γ	Rate of progression from treated human to recovered human
ϕ	Rate at which recovered individuals lose immunity and become susceptible
$\psi_i (i = 1, ..., 3)$	Rate of infected human that are receiving treatment
σ	Progression rate from latent snail to infected snail
σ_1	Progression rate from latent crayfish to infected crayfish
τ	Progression rate from infected snail to dead/incapacitated crayfish
τ_1	Progression rate from infected crayfish to dead/incapacitated crayfish
$N_i (i = h, s, c)$	Total population of human, snail and crayfish respectively

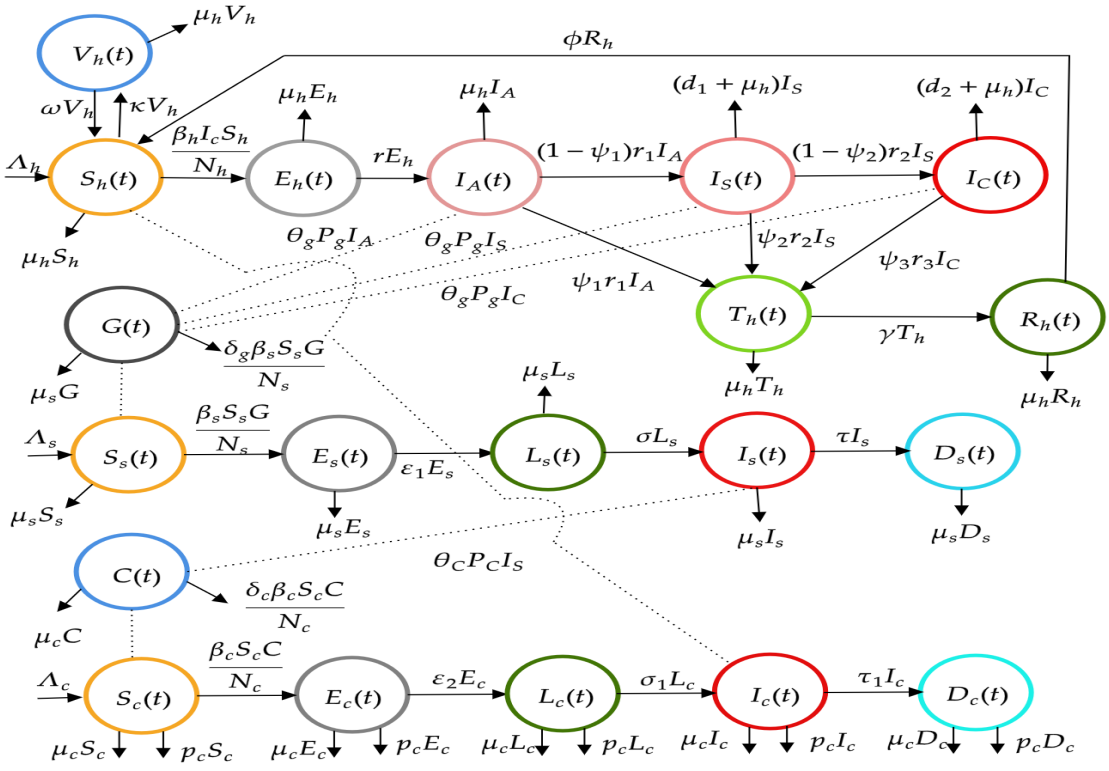

Figure 1. schematic model diagram.

The *Paragonimiasis* model equations with constant control are:

$$
\begin{cases}
\frac{dV_h}{dt} = \kappa S_h - (\omega + \mu_h)V_h \\
\frac{dS_h}{dt} = \Lambda_h + \omega V_h + \phi R_h - \left(\kappa + \frac{\beta_h I_c}{N_h} + \mu_h\right) S_h \\
\frac{dE_h}{dt} = \frac{\beta_h S_h I_c}{N_h} - (r + \mu_h)E_h \\
\frac{dI_A}{dt} = rE_h - (r_1 + \mu_h)I_A \\
\frac{dI_S}{dt} = (1 - \psi_1)r_1 I_A - (r_2 + d_1 + \mu_h)I_S \\
\frac{dI_C}{dt} = (1 - \psi_2)r_2 I_S - (\psi_3 r_3 + d_2 + \mu_h)I_C \\
\frac{dT_h}{dt} = \psi_1 r_1 I_A + \psi_2 r_2 I_S + \psi_3 r_3 I_C - (\gamma + \mu_h)T_h \\
\frac{dR_h}{dt} = \gamma T_h - (\phi + \mu_h)R_h \\
\\
\frac{dG}{dt} = \theta_g P_g (I_A + I_S + I_C) - \left(\frac{\delta_g \beta_s S_s}{N_s} + \mu_g\right) G \\
\\
\frac{dS_s}{dt} = \Lambda_s - \left(\frac{\beta_s G}{N_s} + \mu_s\right) S_s \\
\frac{dE_s}{dt} = \frac{\beta_s S_s G}{N_s} - (\varepsilon_1 + \mu_s)E_s \\
\frac{dL_s}{dt} = \varepsilon_1 E_s - (\sigma + \mu_s)L_s \\
\frac{dI_s}{dt} = \sigma L_s - (\tau + \mu_s)I_s \\
\frac{dD_s}{dt} = \tau I_s - \mu_s D_s \\
\\
\frac{dC}{dt} = \theta_c P_c I_s - \left(\frac{\delta_c \beta_c S_c}{N_c} + \mu_c\right) C \\
\\
\frac{dS_c}{dt} = \Lambda_c - \left(\frac{\beta_c C}{N_c} + p_c + \mu_c\right) S_c \\
\frac{dE_c}{dt} = \frac{\beta_c S_c C}{N_c} - (\varepsilon_2 + p_c + \mu_c)E_c \\
\frac{dL_c}{dt} = \varepsilon_2 E_c - (\sigma_1 + p_c + \mu_c)L_c \\
\frac{dI_c}{dt} = \sigma_1 L_c - (\tau_1 + p_c + \mu_c)I_c \\
\frac{dD_c}{dt} = \tau_1 I_c - (p_c + \mu_c)D_c
\end{cases}
\tag{1}
$$

with the initial conditions:

$$
\begin{cases}
V_h(0 > 0, S_h(0) > 0, E_h(0) \geq 0, I_A(0) \geq 0, I_S(0) \geq 0, I_C(0) \geq 0, T_h(0) \geq 0, R_h(0) \geq 0, G(0) \geq 0, S_s(0) \\
E_s(0) \geq 0, L_s(0) \geq 0, I_s(0) \geq 0, D_s(0) \geq 0, C(0) \geq 0, S_c(0) > 0, E_c(0) \geq 0, L_c(0) \geq 0, I_c(0) \geq 0, D_c(0)
\end{cases}
\tag{2}
$$

2.1 Basic properties of *Paragonimiasis*

Theorem 2.1. *For all* $t > 0$, *the solutions* $V_h, S_h, E_h, I_A, I_S, I_C, T_h, R_h, ..., D_c$ *of the model system (1) with non-negative initial conditions satisfy* $V_h > 0, S_h > 0, E_h > 0, I_A > 0, I_S > 0, I_C > 0, T_h > 0, R_h, .., D_c > 0$. *likewise the region* $\Omega \in \mathbb{R}_+^{20}$ *is attractive and positively invariant with regard to the solution (1).*

To establish Theorem 1 solutions, considering the differential inequality obtained from (1). By the Nagumo–Bony–Brezis theorem on invariant regions (which states that a closed set is positively invariant if the vector field at any boundary point, points inward) Menner (2024), a standard contradiction argument confirms that the non-negative orthant is an invariant region of the system. we demonstrate using exactly the same reasoning that state variables stay non-negative for all $t > 0$ and we obtained:

t_1: $V_h(t_1) = 0, \frac{dV_h}{dt_1} < 0, S_h(t) > 0, E_h(t) > 0, ..., D_c(t) > 0$ for $0 < t < t_1$
t_4: $I_A(t_4) = 0, \frac{dI_A}{dt_4} < 0, S_h(t) > 0, E_h(t) > 0, ..., D_c(t) > 0$ for $0 < t < t_4$
t_5: $I_S(t_5) = 0, \frac{dI_S}{dt_5} < 0, S_h(t) > 0, E_h(t) > 0, ..., D_c(t) > 0$ for $0 < t < t_5$
t_6: $I_C(t_6) = 0, \frac{dI_C}{dt_6} < 0, S_h(t) > 0, E_h(t) > 0, ..., D_c(t) > 0$ for $0 < t < t_6$
t_7: $T_h(t_7) = 0, \frac{dT_h}{dt_7} < 0, S_h(t) > 0, E_h(t) > 0, ..., D_c(t) > 0$ for $0 < t < t_7$
t_8: $R_h(t_8) = 0, \frac{dR_h}{dt_1} < 0, S_h(t) > 0, E_h(t) > 0, ..., D_c(t) > 0$ for $0 < t < t_8$
t_9: $G(t_9) = 0, \frac{dG}{dt_9} < 0, S_h(t) > 0, E_h(t) > 0, ..., D_c(t) > 0$ for $0 < t < t_9$
t_{10}: $S_s(t_{10}) = 0, \frac{dS_s}{dt_{10}} < 0, S_h(t) > 0, E_h(t) > 0, ..., D_c(t) > 0$ for $0 < t < t_{10}$
t_{11}: $E_s(t_{11}) = 0, \frac{dE_s}{dt_{11}} < 0, S_h(t) > 0, E_h(t) > 0, ..., D_c(t) > 0$ for $0 < t < t_{11}$
t_{12}: $L_s(t_{12}) = 0, \frac{dL_s}{dt_{12}} < 0, S_h(t) > 0, E_h(t) > 0, ..., D_c(t) > 0$ for $0 < t < t_{12}$
t_{13}: $I_s(t_{13}) = 0, \frac{dI_s}{dt_{13}} < 0, S_h(t) > 0, E_h(t) > 0, ..., D_c(t) > 0$ for $0 < t < t_{13}$
t_{14}: $D_s(t_{14}) = 0, \frac{dD_s}{dt_{14}} < 0, S_h(t) > 0, E_h(t) > 0, ..., D_c(t) > 0$ for $0 < t < t_{14}$
t_{15}: $C(t_{15}) = 0, \frac{dC}{dt_{15}} < 0, S_h(t) > 0, E_h(t) > 0, ..., D_c(t) > 0$ for $0 < t < t_{15}$
t_{16}: $S_c(t_{16}) = 0, \frac{dS_c}{dt_{16}} < 0, S_h(t) > 0, E_h(t) > 0, ..., D_c(t) > 0$ for $0 < t < t_{16}$
t_{17}: $E_c(t_{17}) = 0, \frac{dE_c}{dt_{17}} < 0, S_h(t) > 0, E_h(t) > 0, ..., D_c(t) > 0$ for $0 < t < t_{17}$
t_{18}: $L_c(t_{18}) = 0, \frac{dL_c}{dt_{18}} < 0, S_h(t) > 0, E_h(t) > 0, ..., D_c(t) > 0$ for $0 < t < t_{18}$
t_{19}: $I_c(t_{19}) = 0, \frac{dI_c}{dt_{19}} < 0, S_h(t) > 0, E_h(t) > 0, ..., D_c(t) > 0$ for $0 < t < t_{19}$
t_{20}: $D_c(t_{20}) = 0, \frac{dD_c}{dt_{20}} < 0, S_h(t) > 0, E_h(t) > 0, ..., D_c(t) > 0$ for $0 < t < t_{20}$.

Therefore, it follows that all solutions of the model equations (1) remain positive for all non-negative initial conditions, thereby satisfying the necessary biological feasibility condition.

Similarly, $\limsup_{t\to\infty} N_h(t) \leq \frac{\Lambda_h}{\mu_h}$, $\limsup_{t\to\infty} N_s(t) \leq \frac{\Lambda_s}{\mu_s}$ and $\limsup_{t\to\infty} N_c(t) \leq \frac{\Lambda_c}{\mu_c}$. In addition, if $N_h(0) \leq \frac{\Lambda_h}{\mu_h}$, $N_s(0) \leq \frac{\Lambda_s}{\mu_s}$,and $N_c(0) \leq \frac{\Lambda_c}{\mu_c}$, then $N_h(t) \leq \frac{\Lambda_h}{\mu_h}$, $N_s(t) \leq \frac{\Lambda_s}{\mu_s}$ and $N_c(t) \leq \frac{\Lambda_c}{\mu_c}$ are the feasible region for system (1):

$$\Omega = \left\{ (N_h, G, N_s, C, N_c) \in \mathbb{R}_+^{20} : N_h(t) \leq \frac{\Lambda_h}{\mu_h}, \quad N_s(t) \leq \frac{\Lambda_s}{\mu_s}, \quad \text{and} \quad N_c(t) \leq \frac{\Lambda_c}{\mu_c} \right\} \quad (3)$$

that (3) is attractive and positively invariant with regard to the system (1).

Proof: Consider the human sub population (N_h) from the system (1), we have the

following

$$\frac{dN_h(t)}{dt} \leq \Lambda_h - \mu_h N_h(t) \tag{4}$$

at $t = 0$, using comparison criterion (4) to get

$$N_h(t) \leq \frac{\Lambda_h}{\mu_h} + \left(N_h(0) - \frac{\Lambda_h}{\mu_h}\right) e^{-\mu_h t}. \tag{5}$$

$$\lim_{t\to\infty} N_h(t) = \frac{\Lambda_h}{\mu_h}. \tag{6}$$

using similar approach for the other sub populations we obtained:
As $t \to \infty$, the limiting bounds for the intermediate host populations satisfy $N_s \to \frac{\Lambda_s}{\mu_s}$, $N_c \to \frac{\Lambda_c}{p_c+\mu_c}$, $G \to \frac{\theta_g P_g \Lambda_h}{\mu_h \mu_g}$, and $C \to \frac{\theta_C P_C \Lambda_s}{\mu_s \mu_C}$. Based on these biological interpretations, system (1) is analyzed within the feasible domain Ω. Furthermore, all state variables $(V_h(t), S_h(t), \ldots, D_c(t))$ remain strictly non-negative for all $t > 0$. Following equation (3), we confirm that Ω is a positively invariant set and a global attractor, ensuring that solutions remain bounded within this manifold. Consequently, Theorem 1 confirms that system (1) is mathematically well-posed and biologically feasible in Ω.

3 *Paragonimiasis* model analysis

This section provides a detailed analytical framework for the *Paragonimiasis* model. We computed the disease-free and endemic equilibrium states, the basic reproduction number (R_0), and analyze the local and global stability of *Paragonimiasis* model at disease free.

3.1 Equilibria states

By setting system (1) to zero, the equilibrium points of system (1) are determined:

$$
\begin{cases}
\frac{dV_h}{dt} = \kappa S_h - (\omega + \mu_h)V_h & = 0 \\
\frac{dS_h}{dt} = \Lambda_h + \omega V_h + \phi R_h - \left(\kappa + \frac{\beta_h I_c}{N_h} + \mu_h\right) S_h & = 0 \\
\frac{dE_h}{dt} = \frac{\beta_h S_h I_c}{N_h} - (r + \mu_h)E_h & = 0 \\
\frac{dI_A}{dt} = rE_h - (r_1 + \mu_h)I_A & = 0 \\
\frac{dI_S}{dt} = (1 - \psi_1)r_1 I_A - (r_2 + d_1 + \mu_h)I_S & = 0 \\
\frac{dI_C}{dt} = (1 - \psi_2)r_2 I_S - (\psi_3 r_3 + d_2 + \mu_h)I_C & = 0 \\
\frac{dT_h}{dt} = \psi_1 r_1 I_A + \psi_2 r_2 I_S + \psi_3 r_3 I_C - (\gamma + \mu_h)T_h & = 0 \\
\frac{dR_h}{dt} = \gamma T_h - (\phi + \mu_h)R_h & = 0 \\
\\
\frac{dG}{dt} = \theta_g P_g (I_A + I_S + I_C) - \left(\frac{\delta_g \beta_s S_s}{N_s} + \mu_g\right) G & = 0 \\
\\
\frac{dS_s}{dt} = \Lambda_s - \left(\frac{\beta_s G}{N_s} + \mu_s\right) S_s & = 0 \\
\frac{dE_s}{dt} = \frac{\beta_s S_s G}{N_s} - (\varepsilon_1 + \mu_s)E_s & = 0 \\
\frac{dL_s}{dt} = \varepsilon_1 E_s - (\sigma + \mu_s)L_s & = 0 \\
\frac{dI_s}{dt} = \sigma L_s - (\tau + \mu_s)I_s & = 0 \\
\frac{dD_s}{dt} = \tau I_s - \mu_s D_s & = 0 \\
\\
\frac{dC}{dt} = \theta_c P_c I_s - \left(\frac{\delta_c \beta_c S_c}{N_c} + \mu_c\right) C & = 0 \\
\\
\frac{dS_c}{dt} = \Lambda_c - \left(\frac{\beta_c C}{N_c} + p_c + \mu_c\right) S_c & = 0 \\
\frac{dE_c}{dt} = \frac{\beta_c S_c C}{N_c} - (\varepsilon_2 + p_c + \mu_c)E_c & = 0 \\
\frac{dL_c}{dt} = \varepsilon_2 E_c - (\sigma_1 + p_c + \mu_c)L_c & = 0 \\
\frac{dI_c}{dt} = \sigma_1 L_c - (\tau_1 + p_c + \mu_c)I_c & = 0 \\
\frac{dD_c}{dt} = \tau_1 I_c - (p_c + \mu_c)D_c & = 0
\end{cases}
\tag{7}
$$

In the absence of *Paragonimiasis*, system (7) admits a disease-free equilibrium (DFE), which characterizes the steady-state of the model in which no infection persists. The local stability of this equilibrium is established by linearizing the system about the DFE and evaluating the corresponding Jacobian matrix. By examining the eigenvalues of the Jacobian, the disease-free equilibrium is locally asymptotically stable whenever all eigenvalues have negative real parts. Hence, the *Paragonimiasis*-free equilibrium of system (7), denoted by E^0 is expressed as:

$$
E^0 = \left(\frac{\kappa\Lambda_h}{(\kappa+\omega+\mu_h)\mu_h}, \frac{\Lambda_h(\omega+\mu_h)}{(\kappa+\omega+\mu_h)\mu_h}, 0,0,0,0,0,0,0,0, \frac{\Lambda_s}{\mu_s}, 0,0,0,0,0, \frac{\Lambda_c}{(p_c+\mu_c)}, 0,0,0,0\right) \tag{8}
$$

Therefore, the total human population at the disease-free equilibrium is:

$$
N_h^0 = S_h^0 + V_h^0 = \frac{\Lambda_h}{\mu_h}. \tag{9}
$$

This result shows that, in the absence of infection, the equilibrium size of the human population depends only on the recruitment rate Λ_h and the natural mortality rate μ_h. Similar population balances can be obtained for the snail and crayfish populations.
The *Paragonimiasis* Present Equilibrium point (PPE), denoted by E^*, is obtain by equating $E_h \neq 0, I_A \neq 0, I_S \neq 0, I_C \neq 0, T_h \neq 0, R_h \neq 0, G \neq 0, E_s \neq 0, L_s \neq 0, I_s \neq 0, D_s \neq 0, C \neq 0, E_c \neq 0, L_c \neq 0, I_c \neq 0, D_c \neq 0$. of the model (1). At equilibrium state, the total population $N^* = V_h^* + S_h^* + E_h^* + I_A^* + I_S^* + ... + D_c^*$, solving system (1) at PPE state yields

$$
\begin{cases}
V_h^* = & \frac{\Lambda_h \kappa K_6}{(K_6K_7K_8)-(\omega\kappa K_6)-\phi\lambda_1\pi_1 K_8}, \\
S_h^* = & \frac{\Lambda_h K_6 K_8}{(K_6K_7K_8)-(\omega\kappa K_6)-(\phi\lambda_1\pi_1 K_8)}, \\
E_h^* = & \frac{\Lambda_h \lambda_1 K_6 K_8}{(K_2K_6K_7K_8)-(\omega\kappa K_2 K_6)-(\phi\lambda_1\pi_1 K_2 K_8)}, \\
I_A^* = & \frac{\Lambda_h \lambda_1 r K_6 K_8}{(K_2K_3K_6K_7K_8)-(\omega\kappa K_2K_3K_6)-(\phi\lambda_1\pi_1 K_2K_3K_8)}, \\
I_S^* = & \frac{(1-\psi_1)\Lambda_h \lambda_1 r r_1 K_6 K_8}{(K_2K_3K_4K_6K_7K_8)-(\omega\kappa K_2K_3K_4K_6)-(\phi\lambda_1\pi_1 K_2K_3K_4K_8)}, \\
I_C^* = & \frac{(1-\psi_1)(1-\psi_2)\Lambda_h \lambda_1 r r_1 r_2 K_6 K_8}{(K_2K_3K_4K_5K_6K_7K_8)-(\omega\kappa K_2K_3K_4K_5K_6)-(\phi\lambda_1\pi_1 K_2K_3K_4K_5K_8)}, \\
T_h^* = & \frac{\Lambda_h \lambda_1 r r_1 K_6 K_8}{K_1K_2K_3[K_6K_7K_8-\omega\kappa K_6-\phi\lambda_1\pi_1 K_8]}\left(\frac{\psi_1}{1}+\frac{(1-\psi_1)\psi_2 r_2}{K_4}+\frac{(1-\psi_1)(1-\psi_2)\psi_3 r_3 r_2}{K_4K_5}\right), \\
R_h^* = & \frac{\Lambda_h \lambda_1 r r_1 \gamma K_8}{K_6K_7K_8-\omega\kappa K_6-\phi\lambda_1 K_8}\left(\frac{\psi_1}{K_1K_2K_3}+\frac{(1-\psi_1)\psi_2 r_2}{K_1K_2K_3K_4}+\frac{(1-\psi_1)(1-\psi_2)\psi_3 r_3 r_2}{K_1K_2K_3K_4K_5}\right), \\
G^* = & \frac{\theta_g P_g}{\mu_g}\left(\frac{\Lambda_h \lambda_1 r K_6 K_8}{(K_2K_3K_6K_7K_8)-(\omega\kappa K_2K_3K_6)-(\phi\lambda_1\pi_1 K_2K_3K_8)}\right) \\
S_s^* = & \frac{\Lambda_s^2 \mu_g}{\mu_s((\beta_s\theta_g P_g\pi_2)+\Lambda_s\mu_g)}, \\
E_s^* = & \frac{\theta_g P_g \Lambda_s \beta_s \pi_2}{K_{11}((\beta_s\theta_g P_g\pi_2)+\Lambda_s\mu_g)}, \\
L_s^* = & \frac{\theta_g P_g \Lambda_s \beta_s \varepsilon_1 \pi_2}{K_{10}.K_{11}((\beta_s\theta_g P_g\pi_2)+\Lambda_s\mu_g)}, \\
I_s^* = & \frac{\theta_g P_g \Lambda_s \beta_s \varepsilon_1 \sigma \pi_2}{K_9.K_{10}.K_{11}((\beta_s\theta_g P_g\pi_2)+\Lambda_s\mu_g)}, \\
D_s^* = & \frac{\tau}{\mu_s}\left(\frac{\theta_g P_g \Lambda_s \beta_s \varepsilon_1 \sigma \pi_2}{K_9.K_{10}.K_{11}((\beta_s\theta_g P_g\pi_2)+\Lambda_s\mu_g)}\right), \\
C^* = & \frac{\theta_c P_c}{\mu_c}\left(\frac{\theta_g P_g \Lambda_s \beta_s \varepsilon_1 \sigma \pi_2}{K_9.K_{10}.K_{11}((\beta_s\theta_g P_g\pi_2)+\Lambda_s\mu_g)}\right), \\
S_c^* = & \frac{\Lambda_c^2 K_9.K_{10}.K_{11}((\beta_s\theta_g P_g\pi_2)+\Lambda_s\mu_g)}{\beta_c\beta_s\Lambda_s\varepsilon_1\sigma\theta_c P_c\theta_g P_g\pi_2}, \\
E_c^* = & \frac{\Lambda_c}{K_{12}}, \\
L_c^* = & \frac{\Lambda_c\varepsilon_2}{K_{12}K_{13}} \\
I_c^* = & \frac{\Lambda_c\varepsilon_2\sigma_1}{K_{12}K_{13}K_{14}} \\
D_c^* = & \frac{\Lambda_c\varepsilon_2\sigma_1\tau_1}{(p_c+\mu_c)K_{12}K_{13}K_{14}}
\end{cases}
\tag{10}
$$

Therefore, (10) define the *Paragonimiasis* Present Equilibrium (PPE), representing the steady state at which the infection persists across all host and compartments.
where,
$K_1 = (\gamma+\mu_h), K_2 = (r+\mu_h), K_3 = (r_1+\mu_h), K_4 = (r_2+d_1+\mu_h), K_5 = (\psi_3 r_3 + d_2 + \mu_h),$
$K_6 = (\phi+\mu_h), K_7 = (\kappa+\lambda_1+\mu_h), K_8 = (\omega+\mu_h),$
$K_9 = (\tau+\mu_s), K_{10} = (\sigma+\mu_s), K_{11} = (\varepsilon_1+\mu_s), K_{12} = (\varepsilon_2+p_c+\mu_c),$
$K_{13} = (\sigma_1+p_c+\mu_c), K_{14} = (\tau_1+p_c+\mu_c),$
$\pi_1 = \frac{\psi_1\gamma r r_1}{(K_1.K_2.K_3)} + \frac{\psi_2\gamma r r_1 r_2(1-\psi_1)}{(K_1.K_2.K_3.K_4)} + \frac{\psi_3\gamma r r_1 r_2 r_3(1-\psi_1)(1-\psi_2)}{(K_1.K_2.K_3.K_4.K_5)}$

$$\pi_2 = \frac{\Lambda_h \lambda_1 r K_6 K_8}{(K_2 K_3 K_6 K_7 K_8) - (\omega \kappa K_2 K_3 K_6) - (\phi \lambda_1 K_2 K_3 K_8)} + \frac{(1-\psi_1) r r_1 \Lambda_h \lambda_1 K_6 K_8}{(K_2 K_3 K_4 K_7 K_8) - (\omega \kappa K_2 K_3 K_6) - (\phi \lambda_1 \pi_1 K_2 K_3 K_8)}$$

3.2 Threshold dynamics/ Basic reproduction number

The basic reproduction number, R_0, represents the average number of secondary infections generated by a single infectious individual in a wholly susceptible population. It is derived for system (1) using the Next Generation Matrix (NGM) method based on the framework of Diekmann et al. (2010). The derivation identifies the infected compartments and dominant transmission pathways to quantify the transmission potential of the disease. The *Paragonimiasis* epidemiological threshold given by $\mathcal{R}_0 = \rho(FV^{-1})$, ρ represents the dominant eigenvalue, F (the new infectious term) and V (the transfer term). For analytical convenience, the model is partitioned into its principal transmission components. Consider the given infectious population:

(X): $\quad E_h,\ I_A,\ I_S,\ I_C, G, E_s, L_s, I_s, C, E_c, L_c, I_c$

The respective R_0 is obtained as:

$$F = \begin{bmatrix} \frac{\beta_h S_h I_C}{N_h} \\ 0 \\ 0 \\ 0 \\ 0 \\ \frac{\beta_s S_s G}{N_s} \\ 0 \\ 0 \\ 0 \\ \frac{\beta_c S_c C}{N_c} \\ 0 \\ 0 \end{bmatrix}, \quad V = \begin{bmatrix} (r+\mu_h)E_h \\ -rE_h + (r_1+\mu_h)I_A \\ -(1-\psi_1)r_1 I_A + (r_2+d_1+\mu_h)I_S \\ -(1-\psi_2)r_2 I_S + (\psi_3 r_3 + d_2 + \mu_h)I_C \\ -\theta_g P_g(I_A + I_S + I_C) + \left(\frac{\delta_g \beta_s S_s}{N_s} + \mu_g\right) G \\ (\varepsilon_1 + \mu_s)E_s \\ -\varepsilon_1 E_s + (\sigma + \mu_s)L_s \\ -\sigma L_s + (\tau + \mu_s)I_s \\ -\theta_c P_c I_s + \left(\frac{\delta_c \beta_c S_c}{N_c} + \mu_c\right) C \\ (\varepsilon_2 + P_c + \mu_c)E_c \\ -\varepsilon_2 E_c + (\sigma_1 + p_c + \mu_c)L_c \\ -\sigma_1 L_c + (\tau_1 + p_c + \mu_c)I_c \end{bmatrix}$$

To obtain the matrices F and V at the *Paragonimiasis*-free equilibrium E^0, we differentiate F and V partially w.r.t each of the infected state variables. Evaluating the resulting Jacobians at the disease-free equilibrium yields:

$$F = \frac{\partial f_i}{\partial x_j} = \begin{bmatrix} 0 & 0 & 0 & 0 & 0 & 0 & 0 & 0 & 0 & 0 & 0 & a_h \\ 0 & 0 & 0 & 0 & 0 & 0 & 0 & 0 & 0 & 0 & 0 & 0 \\ 0 & 0 & 0 & 0 & 0 & 0 & 0 & 0 & 0 & 0 & 0 & 0 \\ 0 & 0 & 0 & 0 & 0 & 0 & 0 & 0 & 0 & 0 & 0 & 0 \\ 0 & 0 & 0 & 0 & 0 & 0 & 0 & 0 & 0 & 0 & 0 & 0 \\ 0 & 0 & 0 & 0 & a_s & 0 & 0 & 0 & 0 & 0 & 0 & 0 \\ 0 & 0 & 0 & 0 & 0 & 0 & 0 & 0 & 0 & 0 & 0 & 0 \\ 0 & 0 & 0 & 0 & 0 & 0 & 0 & 0 & 0 & 0 & 0 & 0 \\ 0 & 0 & 0 & 0 & 0 & 0 & 0 & 0 & 0 & 0 & 0 & 0 \\ 0 & 0 & 0 & 0 & 0 & 0 & 0 & 0 & a_c & 0 & 0 & 0 \\ 0 & 0 & 0 & 0 & 0 & 0 & 0 & 0 & 0 & 0 & 0 & 0 \\ 0 & 0 & 0 & 0 & 0 & 0 & 0 & 0 & 0 & 0 & 0 & 0 \end{bmatrix} \tag{11}$$

where;
$a_h = \frac{\beta_h S_h^0}{N_h^0}$, $a_s = \frac{\beta_s S_s^0}{N_s^0}$ and $a_c = \frac{\beta_c S_c^0}{N_c^0}$

$$V = \frac{\partial v_i}{\partial x_j} = \begin{bmatrix} a_1 & 0 & 0 & 0 & 0 & 0 & 0 & 0 & 0 & 0 & 0 & 0 \\ -r & a_2 & 0 & 0 & 0 & 0 & 0 & 0 & 0 & 0 & 0 & 0 \\ 0 & -b_1 & a_3 & 0 & 0 & 0 & 0 & 0 & 0 & 0 & 0 & 0 \\ 0 & 0 & -b_2 & a_4 & 0 & 0 & 0 & 0 & 0 & 0 & 0 & 0 \\ 0 & -b_3 & -b_4 & -b_5 & a_5 & 0 & 0 & 0 & 0 & 0 & 0 & 0 \\ 0 & 0 & 0 & 0 & 0 & a_6 & 0 & 0 & 0 & 0 & 0 & 0 \\ 0 & 0 & 0 & 0 & 0 & -\varepsilon_1 & a_7 & 0 & 0 & 0 & 0 & 0 \\ 0 & 0 & 0 & 0 & 0 & 0 & -\sigma & a_8 & 0 & 0 & 0 & 0 \\ 0 & 0 & 0 & 0 & 0 & 0 & 0 & -b_6 & a_9 & 0 & 0 & 0 \\ 0 & 0 & 0 & 0 & 0 & 0 & 0 & 0 & 0 & a_{10} & 0 & 0 \\ 0 & 0 & 0 & 0 & 0 & 0 & 0 & 0 & 0 & -\varepsilon_2 & a_{11} & 0 \\ 0 & 0 & 0 & 0 & 0 & 0 & 0 & 0 & 0 & 0 & -\sigma 1 & a_{12} \end{bmatrix} \tag{12}$$

where;
$a_1 = (r + \mu_h)$, $a_2 = (r_1 + \mu_h)$, $a_3 = (r_2 + d_1 + \mu_h)$, $a_4 = (\psi_3 r_3 + d_2 + \mu_h))$, $a_5 = \left(\frac{\delta_g \beta_s S_s}{N_s} + \mu_g\right) G$, $a_6 = (\varepsilon_1 + \mu_s)$, $a_7 = (\sigma + \mu_s)$, $a_8 = (\tau + \mu_s)$, $a_9 = \left(\frac{\delta_c \beta_c S_c}{N_c} + \mu_c\right)$, $a_{10} = (\varepsilon_2 + p_c + \mu_c)$, $a_{11} = (\sigma_1 + p_c + \mu_c)$, and $a_{12} = (\tau_1 + p_c + \mu_c)$.
$b_1 = (1 - \psi_1) r_1$, $b_2 = (1 - \psi_2) r_2$, $b_3 = \theta_g P_g$, $b_4 = \theta_g P_g$, $b_5 = \theta_g P_g$ and $b_6 = \theta_c P_c$.

Taking the inverse of equation (12) we have:

$$\mathrm{V}^{-1} = \begin{bmatrix} \frac{1}{a_1} & 0 & 0 & 0 & 0 & 0 & 0 & 0 & 0 & 0 & 0 & 0 \\ \frac{r}{a_1 a_2} & \frac{1}{a_2} & 0 & 0 & 0 & 0 & 0 & 0 & 0 & 0 & 0 & 0 \\ \frac{r b_1}{a_1 a_2 a_3} & \frac{b_1}{a_2 a_3} & \frac{1}{a_3} & 0 & 0 & 0 & 0 & 0 & 0 & 0 & 0 & 0 \\ \frac{r b_1 b_2}{a_1 a_2 a_3 a_4} & \frac{b_1 b_2}{a_2 a_3 a_4} & \frac{b_2}{a_3 a_4} & \frac{1}{a_4} & 0 & 0 & 0 & 0 & 0 & 0 & 0 & 0 \\ \frac{r a_3 a_4 b_3 + r b_1 a_4 b_4 + r b_1 b_2 b_5}{a_1 a_2 a_3 a_4 a_5} & \frac{a_3 a_4 b_3 + b_1 a_4 b_4 + b_1 b_2 b_5}{a_2 a_3 a_4 a_5} & \frac{a_4 b_4 + b_2 b_5}{a_3 a_4 a_5} & \frac{b_5}{a_4 a_5} & \frac{1}{a_5} & 0 & 0 & 0 & 0 & 0 & 0 & 0 \\ 0 & 0 & 0 & 0 & 0 & \frac{1}{a_6} & 0 & 0 & 0 & 0 & 0 & 0 \\ 0 & 0 & 0 & 0 & 0 & \frac{\varepsilon_1}{a_6 a_7} & \frac{1}{a_7} & 0 & 0 & 0 & 0 & 0 \\ 0 & 0 & 0 & 0 & 0 & \frac{\sigma \varepsilon_1}{a_6 a_7 a_8} & \frac{\sigma}{a_7 a_8} & \frac{1}{a_8} & 0 & 0 & 0 & 0 \\ 0 & 0 & 0 & 0 & 0 & \frac{\sigma \varepsilon_1 b_6}{a_6 a_7 a_8 a_9} & \frac{\sigma b_6}{a_7 a_8 a_9} & \frac{b_6}{a_8 a_9} & \frac{1}{a_9} & 0 & 0 & 0 \\ 0 & 0 & 0 & 0 & 0 & 0 & 0 & 0 & 0 & \frac{1}{a_{10}} & 0 & 0 \\ 0 & 0 & 0 & 0 & 0 & 0 & 0 & 0 & 0 & \frac{\varepsilon_2}{a_{10} a_{11}} & \frac{1}{a_{11}} & 0 \\ 0 & 0 & 0 & 0 & 0 & 0 & 0 & 0 & 0 & \frac{\sigma_1 \varepsilon_2}{a_{10} a_{11} a_{12}} & \frac{\sigma_1}{a_{11} a_{12}} & \frac{1}{a_{12}} \end{bmatrix} \tag{13}$$

Thus,

$$F_h V_h^{-1} = \begin{bmatrix} 0 & 0 & 0 & 0 & 0 & 0 & 0 & 0 & 0 & 0 & 0 & \frac{a_h}{a_1} \\ 0 & 0 & 0 & 0 & 0 & 0 & 0 & 0 & 0 & 0 & 0 & \frac{ra_h}{a_1a_2} \\ 0 & 0 & 0 & 0 & 0 & 0 & 0 & 0 & 0 & 0 & 0 & \frac{rb_1a_h}{a_1a_2a_3} \\ 0 & 0 & 0 & 0 & 0 & 0 & 0 & 0 & 0 & 0 & 0 & \frac{rb_1b_2a_h}{a_1a_2a_3a_4} \\ 0 & 0 & 0 & 0 & 0 & 0 & 0 & 0 & 0 & 0 & 0 & \frac{a_h(ra_3a_4b_3+rb_1a_4b_4+rb_1b_2b_5)}{a_1a_2a_3a_4a_5} \\ 0 & 0 & 0 & 0 & \frac{a_s}{a_6} & 0 & 0 & 0 & 0 & 0 & 0 & 0 \\ 0 & 0 & 0 & 0 & \frac{\varepsilon_1 a_s}{a_6a_7} & 0 & 0 & 0 & 0 & 0 & 0 & 0 \\ 0 & 0 & 0 & 0 & \frac{\sigma\varepsilon_1 a_s}{a_6a_7a_8} & 0 & 0 & 0 & 0 & 0 & 0 & 0 \\ 0 & 0 & 0 & 0 & \frac{\sigma\varepsilon_1 b_6 a_s}{a_6a_7a_8a_9} & 0 & 0 & 0 & 0 & 0 & 0 & 0 \\ 0 & 0 & 0 & 0 & 0 & 0 & 0 & 0 & \frac{a_c}{a_{10}} & 0 & 0 & 0 \\ 0 & 0 & 0 & 0 & 0 & 0 & 0 & 0 & \frac{\varepsilon_2 a_c}{a_{10}a_{11}} & 0 & 0 & 0 \\ 0 & 0 & 0 & 0 & 0 & 0 & 0 & 0 & \frac{\sigma_1\varepsilon_2 a_c}{a_{10}a_{11}a_{12}} & 0 & 0 & 0 \end{bmatrix} \tag{14}$$

The spectral radius $\rho(FV^{-1}) = R_0$. Therefore, the basic reproduction number for *Paragonimiasis*, which is the dominant eigenvalue is given as:

$$\begin{aligned} R_0 = \Bigg[& \left(\frac{\beta_h(\omega+\mu_h)}{\kappa+\omega+\mu_h}\right)(\theta_g P_g)\left(\frac{\beta_s\Lambda_s}{\mu_s N_s^0}\right)(\theta_c P_c)\left(\frac{\beta_c\Lambda_c}{(p_c+\mu_c)N_c^0}\right) \\ & \times \frac{r(1-\psi_1)r_1(1-\psi_2)r_2}{(r+\mu_h)(r_1+\mu_h)(r_2+d_1+\mu_h)(\psi_3 r_3+d_2+\mu_h)} \\ & \times \frac{\varepsilon_1\sigma}{(\varepsilon_1+\mu_s)(\sigma+\mu_s)(\tau+\mu_s)} \times \frac{\varepsilon_2\sigma_1}{(\varepsilon_2+p_c+\mu_c)(\sigma_1+p_c+\mu_c)(\tau_1+p_c+\mu_c)} \\ & \times \frac{1}{\left(\frac{\delta_g\beta_s S_s^0}{N_s^0}+\mu_g\right)\left(\frac{\delta_c\beta_c S_c^0}{N_c^0}+\mu_c\right)} \Bigg]^{\frac{1}{3}} \end{aligned} \tag{15}$$

at DFE all infected compartments are equated to zero, only the susceptible compartments are at steady states i.e,
$S_h^0 = N_h^0 = \frac{\Lambda_h}{\mu_h}$, $\frac{S_h^0}{N_h^0} = \frac{(\omega+\mu_h)}{\kappa+\omega+\mu_h}$, $S_s^0 = N_s^0 = \frac{\Lambda_s}{\mu_s}$ and $S_c^0 = N_c^0 = \frac{\Lambda_h}{(p_c-\mu_h)}$, Therefore;

$$R_0 = \left[\left(\frac{(\theta_g P_g)(\theta_C P_C)\beta_s \beta_c}{(\delta_g \beta_s + \mu_g)\,(\delta_c \beta_c + \mu_c)} \right) \left(\frac{\beta_h(\omega + \mu_h)}{\kappa + \omega + \mu_h} \right) \right.$$
$$\times \frac{r(1-\psi_1)r_1(1-\psi_2)r_2}{(r+\mu_h)(r_1+\mu_h)(r_2+d_1+\mu_h)(\psi_3 r_3 + d_2 + \mu_h)}$$
$$\left. \times \frac{\varepsilon_1 \sigma}{(\varepsilon_1 + \mu_s)(\sigma + \mu_s)(\tau + \mu_s)} \times \frac{\varepsilon_2 \sigma_1}{(\varepsilon_2 + p_c + \mu_c)(\sigma_1 + p_c + \mu_c)(\tau_1 + p_c + \mu_c)} \right]^{\frac{1}{3}} \tag{16}$$

3.3 Global stability for *Paragonimiasis*-free equilibrium

To investigate the global asymptotic stability of the *Paragonimiasis*-free equilibrium in system (1), we apply the methodology proposed in Castillo et al. (2002). This framework offers adequate criteria for proving the global stability of the disease-free equilibrium.

Lemma 3.1. *writing system (1) in the form*

$$\begin{cases} \frac{dX}{dt} & = F(X, Z) \\ \frac{dZ}{dt} & = G(X, Z,), (X, 0) = 0 \end{cases} \tag{17}$$

where $X = (V_h, S_h, T_h, R_h, S_s, D_s, S_c, D_c)$ *and* $Z = (E_h, I_A, I_S, I_C, G, E_s, L_s, I_s, C, E_c, L_c, I_c,)$ *and components of* $X \in \mathbb{R}^8$ *represent the population that are not infected and components of* $Z \in \mathbb{R}^{12}$ *represent the population that are infected Castillo et al. (2002). Giving the Paragonimiasis-free equilibrium as* $E^0 = (X^0, 0)$*, where*

$$X^0 = \left(\frac{\kappa \Lambda_h}{(\kappa + \omega + \mu_h)\mu_h}, \frac{\Lambda_h(\omega + \mu_h)}{(\kappa + \omega + \mu_h)\mu_h}, 0, 0, 0, 0, 0, 0, 0, \frac{\Lambda_s}{\mu_s}, 0, 0, 0, 0, 0, \frac{\Lambda_c}{(p_c + \mu_c)}, 0, 0, 0, 0 \right) \tag{18}$$

The conditions outlined below are necessary to guarantee global asymptotic stability:
$H_1 : \frac{dX}{dt} = F(X^0, 0)$, X^0 *is (GAS.*
$H_2 : G(X, Z) = AZ - \hat{G}(X, Z), \hat{G}(X, Z) \geq 0$ *for* $(X, Z) \in \Omega$*, where* $A = D_z G(X^0, 0)$ *is an M-matrix and* Ω *is the biological feasible region. Hence,* E^0 *is (GAS) if* $R_0 < 1$*.*

Theorem 3.2. *The Paragonimiasis free equilibrium state at DFE is globally asymptotically stable when* $R_0 < 1$ *and the following two requirements are met.*

Proof: Recall that

$$X = (V_h, S_h, T_h, R_h, S_s, D_s, S_c, D_c)^T)$$
$$Z = (E_h, I_A, I_S, I_C, G, E_s, L_s, I_s, C, E_c, L_c, I_c,)^T$$

$$H(X,Z) = \begin{pmatrix} \kappa S_h - (\omega + \mu_h)V_h \\ \Lambda_h + \omega V_h + \phi R_h - (\kappa + \mu_h)S_h, \\ -(\gamma + \mu_h)T_h \\ \gamma T_h - (\phi + \mu_h)R_h \\ \Lambda_s - \mu_s S_s \\ -\mu_s D_s \\ \Lambda_c - (p_c + \mu_c)S_c \\ -(p_c + \mu_c)D_c. \end{pmatrix} \tag{19}$$

$$H(X,0) = \begin{pmatrix} \kappa S_h - (\omega + \mu_h)V_h \\ \Lambda_h + (\kappa + \mu_h)S_h, \\ 0 \\ 0 \\ \Lambda_s - \mu_s S_s \\ 0 \\ \Lambda_c - (p_c + \mu_c)S_c \\ 0 \end{pmatrix} \tag{20}$$

Solving for equation (20) using IF Yielded:

$$\text{As } t \to \infty, \quad V_h(t) = \frac{\kappa \Lambda_h}{(\kappa + \omega + \mu_h)\mu_h} \tag{21}$$

$$\text{As } t \to \infty, S_h(t) \to \frac{\Lambda_h(\omega + \mu_h)}{(\kappa + \omega + \mu_h)\mu_h} \tag{22}$$

$$\text{As } t \to \infty, S_s(t) \to \frac{\Lambda_s}{\mu_s} \tag{23}$$

$$\text{As } t \to \infty, S_c(t) \to \frac{\Lambda_c}{p_c + \mu_c} \tag{24}$$

Therefore, Condition (H_1) of the Castillo-Chavez stability criterion for (GAS) is satisfied.

Recall that $H_2 : G(X,Z) = AZ - \hat{G}(X,Z)$,

$$G(X,Z)=\begin{pmatrix}\frac{\beta_h S_h I_c}{N_h}-(r+\mu_h)E_h\\ rE_h-(r_1+\mu_h)I_A\\ (1-\psi_1)r_1I_A-(r_2+d_1+\mu_h)I_S\\ (1-\psi_2)r_2I_S-(\psi_3 r_3+d_2+\mu_h)I_C\\ \theta_g P_g(I_A+I_S+I_C)-\left(\frac{\delta_g\beta_s S_s}{N_s}+\mu_g\right)G\\ \frac{\beta_s S_s G}{N_s}-(\varepsilon_1+\mu_s)E_s\\ \varepsilon_1 E_s-(\sigma+\mu_s)L_s\\ \sigma L_s-(\tau+\mu_s)I_s\\ \theta_c P_c I_s-\left(\frac{\delta_c\beta_c S_c}{N_c}+\mu_c\right)C\\ \frac{\beta_c S_c C}{N_c}-(\varepsilon_2+p_c+\mu_c)E_c\\ \varepsilon_2 E_c-(\sigma_1+p_c+\mu_c)L_c\\ \sigma_1 L_c-(\tau_1+p_c+\mu_c)I_c\end{pmatrix} \tag{25}$$

where
$A=D_Z G(X^*,0)$ is an M-matrix (all off-diagonal entries are non-negative) and $\widehat{G}(X,Z)\geq 0$. Hence, for the infected compartment state vector:
$Z=(E_h,I_A,I_S,I_C,G,E_s,L_s,I_s,C,E_c,L_c,I_c)^T$, the linearized infected subsystem at the DFE becomes: $\frac{dZ}{dt}=AZ$, where the structural matrix A is defined as the linearized infected subsystem at the DFE.

$$A=\begin{pmatrix}-e_1 & 0 & 0 & 0 & 0 & 0 & 0 & 0 & 0 & 0 & 0 & \beta_h\frac{S_h^0}{N_h^0}\\ r & -e_2 & 0 & 0 & 0 & 0 & 0 & 0 & 0 & 0 & 0 & 0\\ 0 & m_1 & -e_3 & 0 & 0 & 0 & 0 & 0 & 0 & 0 & 0 & 0\\ 0 & 0 & m_2 & -e_4 & 0 & 0 & 0 & 0 & 0 & 0 & 0 & 0\\ 0 & \theta_g P_g & \theta_g P_g & \theta_g P_g & -\mu_g & 0 & 0 & 0 & 0 & 0 & 0 & 0\\ 0 & 0 & 0 & 0 & \beta_s\frac{S_s^0}{N_s^0} & -e_5 & 0 & 0 & 0 & 0 & 0 & 0\\ 0 & 0 & 0 & 0 & 0 & \varepsilon_1 & -e_6 & 0 & 0 & 0 & 0 & 0\\ 0 & 0 & 0 & 0 & 0 & 0 & \sigma & -e_7 & 0 & 0 & 0 & 0\\ 0 & 0 & 0 & \theta_c P_c & 0 & 0 & 0 & 0 & -\mu_c & 0 & 0 & 0\\ 0 & 0 & 0 & 0 & 0 & 0 & 0 & 0 & \beta_c\frac{S_c^0}{N_c^0} & -e_8 & 0 & 0\\ 0 & 0 & 0 & 0 & 0 & 0 & 0 & 0 & 0 & \varepsilon_2 & -e_9 & 0\\ 0 & 0 & 0 & 0 & 0 & 0 & 0 & 0 & 0 & 0 & \sigma_1 & -e_{10}\end{pmatrix} \tag{26}$$

where;
$e_1=(r+\mu_h)$, $e_2=(r_1+\mu_h)$, $e_3=(r_2+d_1+\mu_h)$, $e_4=(\psi_3 r_3+d_2+\mu_h)$, $e_5=(\varepsilon_1+\mu_s)$, $e_6=(\sigma+\mu_s)$, $e_7=(\tau+\mu_s)$, $e_8=(\varepsilon_2+p_c+\mu_c)$, $e_9=(\sigma_1+p_c+\mu_c)$, $e_{10}=(\tau_1+p_c+\mu_c)$, $m_1=(1-\psi_1)r_1$, $m_2=(1-\psi_2)r_2$

All off-diagonal entries are non-negative; hence A is verified to be a Metzler matrix. Recall that the infected subsystem can be expressed as $G(X,Z)=AZ-\widehat{G}(X,Z)$, solving the system, we obtained:

$$AZ - G(X,Z) = \begin{pmatrix} \beta_h I_c \left(\frac{S_h^0}{N_h^0} - \frac{S_h}{N_h} \right) \\ 0 \\ 0 \\ 0 \\ \frac{\delta_g \beta_s S_s G}{N_s} \\ \beta_s G \left(\frac{S_s^0}{N_h^0} - \frac{S_s}{N_s} \right) \\ \\ 0 \\ 0 \\ \frac{\delta_c \beta_c S_c C}{N_c} \\ \beta_c C \left(\frac{S_c^0}{N_c^0} - \frac{S_c}{N_c} \right) \\ \\ 0 \\ 0 \end{pmatrix} \tag{27}$$

$$G(X,Z) = \begin{pmatrix} \hat{G}_1(X,Z) \\ \hat{G}_2(X,Z) \\ \hat{G}_3(X,Z) \\ \hat{G}_4(X,Z) \\ \hat{G}_5(X,Z) \\ \hat{G}_6(X,Z) \\ \hat{G}_7(X,Z) \\ \hat{G}_8(X,Z) \\ \hat{G}_9(X,Z) \\ \hat{G}_{10}(X,Z) \\ \hat{G}_{11}(X,Z) \\ \hat{G}_{12}(X,Z) \end{pmatrix} = \begin{pmatrix} \beta_h I_c \left(\frac{S_h^0}{N_h^0} - \frac{S_h}{N_h} \right) \\ 0 \\ 0 \\ 0 \\ \frac{\delta_g \beta_s S_s G}{N_s} \\ \beta_s G \left(\frac{S_s^0}{N_h^0} - \frac{S_s}{N_s} \right) \\ \\ 0 \\ 0 \\ \frac{\delta_c \beta_c S_c C}{N_c} \\ \beta_c C \left(\frac{S_c^0}{N_c^0} - \frac{S_c}{N_c} \right) \\ \\ 0 \\ 0 \end{pmatrix} \tag{28}$$

Since $\hat{G}_1(X,Z), \hat{G}_2(X,Z), \hat{G}_3(X,Z), \hat{G}_4(X,Z), \hat{G}_6(X,Z), \hat{G}_7(X,Z), \hat{G}_8(X,Z), \hat{G}_{10}(X,Z), \hat{G}_{11}(X,Z), \hat{G}_{12}(X,Z) \geq 0$ also, $\frac{S_h}{N_h} \leq \frac{S_h^0}{N_h^0}$, $\frac{S_s}{N_s} \leq \frac{S_s^0}{N_s^0}$, and $\frac{S_c}{N_c} \leq \frac{S_h^c}{N_c^0}$ and $\hat{G}_5(X,Z), \hat{G}_9(X,Z) \geq 0$ and $S_s \geq 0$, $G \geq 0$ and $S_c \geq 0$ $C \geq 0$ are within the feasible region. Thus, the non-negativity condition in (H_2) is satisfied. Since condition (H_1) has also been established,

all the hypotheses of the Castillo-Chavez, Feng, and Huang (2002) theorem are fulfilled. Therefore, whenever $R_0 < 1$, the PFE of the model is GAS in the feasible region Ω.

3.4 Sensitivity analysis of *Paragonimiasis* model parameters

The model's key parameters were subjected to a sensitivity analysis to determine their influence on the basic reproduction number R_0 in the *Paragonimiasis* transmission dynamics. The sensitivity indices were determined by partially differentiating R_0 with respect to each parameter in model equation (16), using the method described in Section 2. The normalized forward sensitivity index for a parameter χ was calculated using $\gamma_{\chi}^{R_0} = \frac{\partial R_0}{\partial \chi} \cdot \frac{\chi}{R_0}$, and every parameter in R_0 was subjected to the same methodology and it was observed that the parameters in table 2 driven by parameters associated with disease transmission, infection progression, and environmental shedding. The transmission parameters β_h, β_s, and β_c, together with r, r_1, θ_g, P_g, θ_c, and P_c, recorded the highest positive sensitivity indices of approximately $+0.33$. This suggests that increases in these parameters can substantially enhance the spread and persistence of the disease. The parameters r_2 and ε_2 also showed appreciable positive effects, with sensitivity indices of $+0.29$ and $+0.27$, respectively, whereas ε_1 and r_3 had comparatively small positive effects. In contrast, the vaccination rate, κ, had a negative sensitivity index of -0.08, indicating that increasing vaccination coverage contributes to a reduction in R_0, although the effect is relatively limited. Overall, the findings emphasize the importance of reducing transmission and environmental contamination, promoting early detection and treatment, and disrupting the snail–crayfish–human transmission pathway. Therefore, a coordinated control strategy that simultaneously targets several highly sensitive parameters is likely to be more effective than relying on a single intervention. The sensitivity analysis results also shows that the progression of infection within snails is the strongest positive contributor to R_0, with σ recording a sensitivity index of $+0.35$. On the other hand, several parameters have negative sensitivity indices, notably the natural human mortality rate μ_h (-1.10), crayfish mortality or harvesting rate p_c (-0.25), and the treatment rates ψ_3, ψ_2, and ψ_1. The negative indices associated with the treatment parameters indicate that prompt and effective treatment of infected individuals can contribute to reducing disease transmission. However, the negative sensitivity of μ_h should not be taken to imply that increasing human mortality is a control measure; instead, it reflects the importance of shortening the duration of infection and reducing the amount of infectious material released into the environment. The results obtained strongly suggest that effective control of *Paragonimiasis* should combine interventions that slow snail infection progression, regulate crayfish availability, improve treatment of infected individuals, and reduce human contamination of the environment.

Table 2. Sensitivity indices for *Paragonimiasis* model $\mathcal{R}_0$

.

Parameter	Baseline values	References	Sensitivity Index	Remarks
β_h	0.000969	Yuang et al. (2018)	0.3333	Positive
ω	0.3	Assumed	0.0181	Positive
κ	0.5	Assumed	-0.0784	Negative
θ_g	$1 \times 10^{-}2$	Yuang et al. (2018)	0.3333	Positive
θ_c	0.1564	Yuang et al. (2018)	0.3333	Positive
P_g	1.46×10^{6}	Yuang et al. (2018)	0.3333	Positive
P_c	452	Yuang et al. (2018)	0.3333	Positive
r	0.2405	Yakoko et al. (2024)	0.3268	Positive
r_1	0.0111	Chen et al. (2011)	0.3297	Positive
r_2	0.01667	Assumed	0.2954	Positive
r_3	0.001	Assumed	-0.0001	Negative
ψ_1	0.083	Stauch (2011)	-0.0302	Negative
ψ_2	0.333	Stauch (2011)	-0.1664	Negative
ψ_3	0.033	Stauch (2011)	-0.0001	Negative
d_1	0.1	Yakoko et al. (2024)	-0.2045	Negative
d_2	0.12	Yakoko et al. (2024)	-0.1176	Negative
μ_h	0.00014	Yakoko et al. (2024)	-1.0528	Negative
β_s	3.12×10^{-3}	Yuang et al. (2018)	0.3325	Positive
ε_1	0.234	Yakoko et al. (2024)	0.0266	Positive
σ	1	Stauch (2011)	0.3391	Positive
τ	0.001	Rahman (2010)	-0.0467	Negative
μ_s	0.203	Yuang et al. (2018)	-0.0810	Negative
β_c	3.59	Yuang et al. (2018)	0.3333	Positive
ε_2	0.65	Yakoko et al. (2024)	0.2726	Positive
σ_1	0.690	Yakoko et al. (2024)	-0.0068	Negative
τ_1	0.3	Islam et al. (2013)	-0.0993	Negative
p_c	452	Yuang et al. (2018)	-0.0928	Negative
μ_c	2.614	Yuang et al. (2018)	-0.0001	Negative

4 Numerical simulations

This section presents the numerical simulation results illustrated in Figures 1(a–d), 2(e–h), 3(i–l), 4(m–p), and 5(q–t), which describe the time-dependent behaviour of the various compartments in the *Paragonimiasis* transmission model. The discussion focuses on the evolution of each epidemiological class over the simulation period, highlighting the effects of providing a clearer understanding of how infection is transmitted, reduced, and eventually controlled within the modeled populations.

Table 3. Initial values for the variables.

Variables	Description	Values	Sources
$V_h(0)$	Vaccinated humann at time t	50	Assumed
$S_h(0)$	Susceptible human at time t	1.9×10^5	Yuang et al. (2018)
$E_h(0)$	Exposed human at time t	2,882	Yuang et al. (2018)
$I_A(0)$	Asymptomatic infected human at t	360	Yakoko et al. (2024)
$I_S(0)$	Symptomatic infected human at time t	450	Assumed
$I_C(0)$	Chronically infected human at time t	430	Yakoko et al. (2024)
$T_h(0)$	Treated human at time t	510	Assumed
$R_h(t)$	Recovered human at time t	568	Yuang et al. (2018)
$G(t)$	Embryonated eggs at time t	25	Yuang et al. (2018)
$S_s(t)$	Susceptible snail at time t	5×10^5	Assumed
$E_s(t)$	Exposed snail at time t	20	Yakoko et al. (2024)
$L_s(0)$	Latent snail at time t	25	Assumed
$I_s(t)$	Infected snail at time t	12	Yuang et al. (2018)
$D_s(t)$	Dead/incapacitated snail at time t	5	Assumed
$C(t)$	Number of cercariae at a given time t	14	Yuang et al. (2018)
$S_c(t)$	Susceptible crayfish at time t	9.99	Yuang et al. (2018)
$E_c(t)$	Exposed crayfish at time t	2.13	Yakoko et al. (2024)
$L_c(t)$	Latent crayfish at time t	14	Assumed
$I_c(t)$	Infected crayfish at time t	1.9	Yuang et al. (2018)
$D_c(t)$	Dead/incapacitated crayfish at time t	1.9	dye (1996)

4.1 Behavior of V_h, S_h,E_h and I_A plotted against time (week).

This Figures 1(a–d), demonstrate the effectiveness of the recommended intervention strategies in preventing the development of *Paragonimiasis*. As seen by the rapid decline of symptomatically infected, chronically infected, treated, and recovered populations to negligible levels, the combined interventions successfully suppress current infections, eliminate chronic cases, and reduce the need for extended treatment. These findings suggest that regular immunization, early diagnosis, effective treatment, and other suitable management strategies might greatly reduce the incidence of *Paragonimiasis* and establish ideal conditions for its eventual elimination. This aligns closely with the work of Huang

(2020), they developed a multi-group dynamic transmission model for Clonorchis sinensis and found that combinations of interventions such as preventive chemo and environmental modification were substantially more beneficial than single measures applied in isolation. Their work underscores the importance of sustained, combined strategies for achieving infection control, this supported our findings on integrating interventions which can interrupt *Paragonimiasis* transmission.

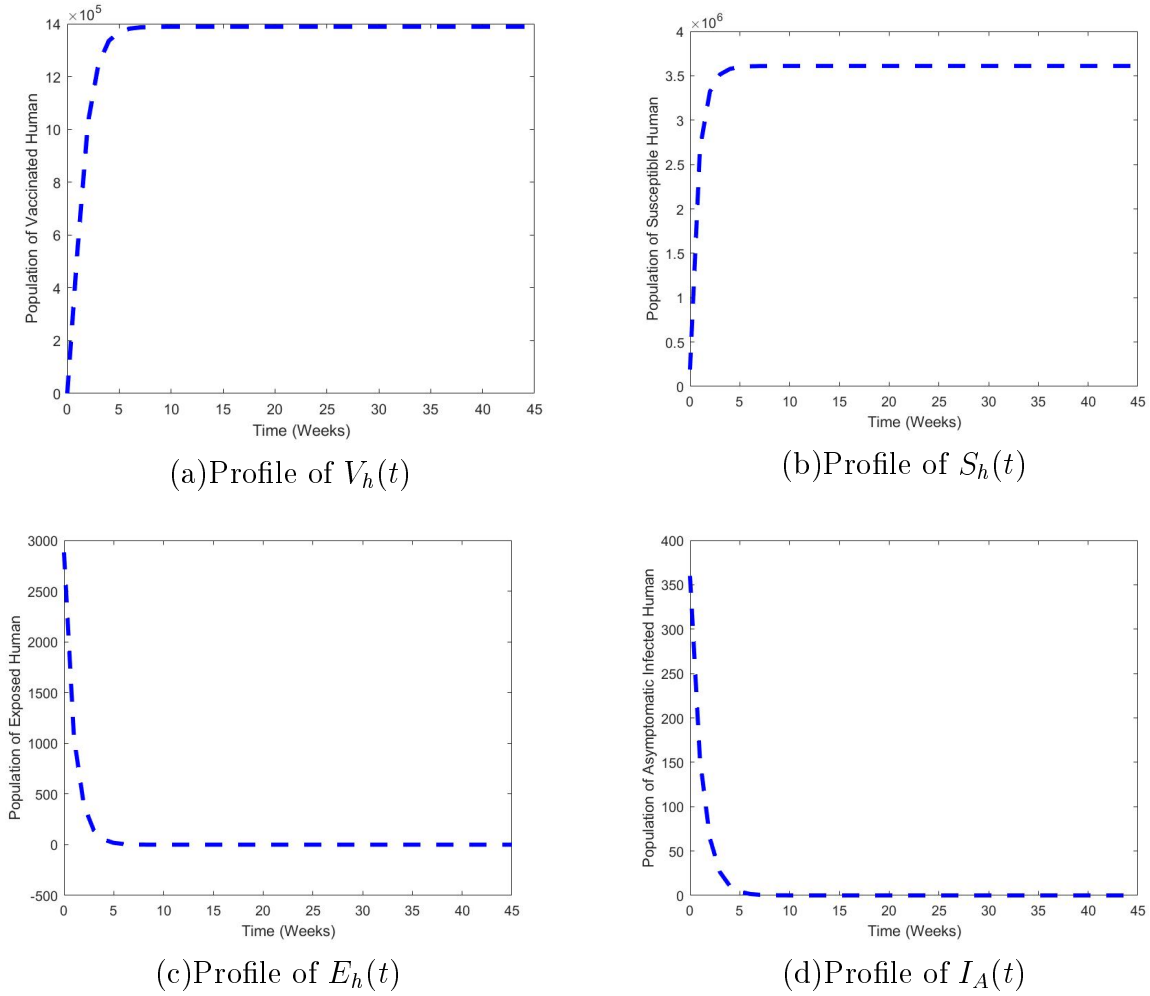

(a)Profile of $V_h(t)$ (b)Profile of $S_h(t)$

(c)Profile of $E_h(t)$ (d)Profile of $I_A(t)$

Figure 1: Dynamics of V_h, S_h, E_h and I_A population against time (week).

4.2 Behavior of I_S, I_C, T_h and R_h plotted against time (week).

The dependent trajectories of the symptomatically infected (I_S), chronically infected (I_C), treated (T_h), and recovered (R_h) human compartments are illustrated in Figures 2(e–h). Over the initial five-week period, all four compartments experience a sharp decline, subsequently remaining near zero throughout the rest of the simulation. Specifically, the symptomatic and chronic infection classes plummet from initial levels of approximately 450 and 430 individuals, respectively, to near-elimination. This dramatic drop demonstrates that integrating vaccination, prompt diagnosis, and effective therapeutic interventions markedly suppresses both acute and persistent disease stages. Concurrently, the treated compartment decreases from around 510 individuals to negligible levels, reflecting a diminishing demand for clinical care as new infections drop. The recovered population similarly contracts from roughly 560 to minimal levels due to the reduced

influx of infected individuals moving through the recovery pipeline. Collectively, these findings confirm that the evaluated control strategies successfully interrupt transmission and mitigate the overall burden of *Paragonimiasis*, consistent with observations by Edward (2025) regarding the impact of proactive preventive measures in disease control.

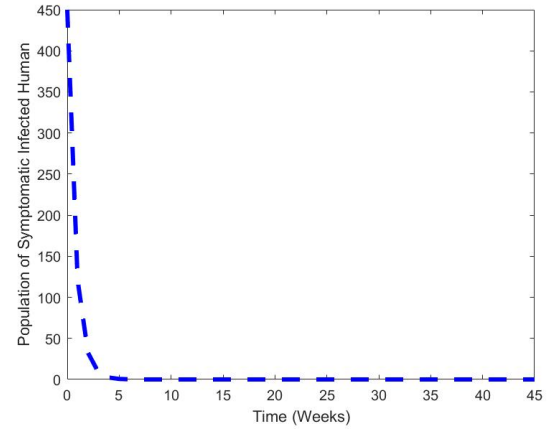

(e)Profile of $I_S(t)$

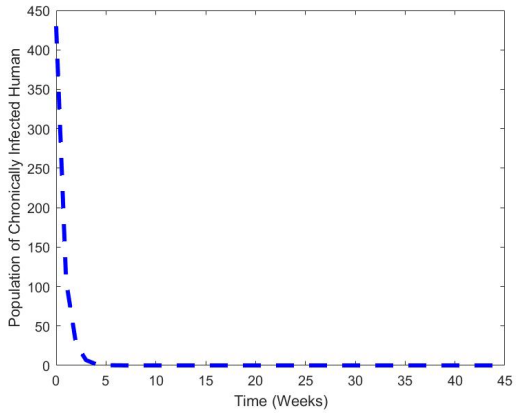

(f)Profile of $I_C(t)$

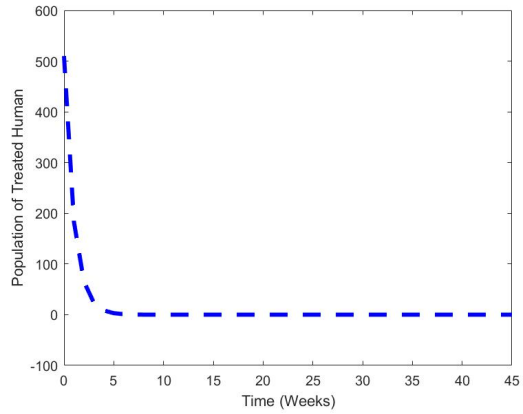

(g)Profile of $T_h(t)$

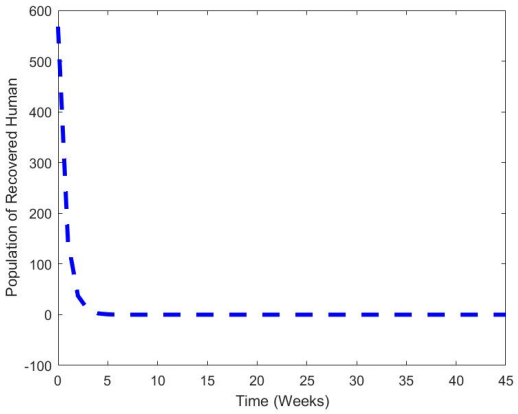

(h)Profile of $R_h(t)$

Figure 2: Dynamics of I_S, I_C,T_h and R_h population against time (week).

4.3 Behavior of G, S_s,E_s and L_s plotted against time (week).

The 45-week simulation trajectories of the parasite egg population (G), susceptible snail population (S_s), exposed snail population (E_s), and latent snail population (L_s) are presented in Figures 3(i–l). The parasite egg population initially increases sharply before gradually declining, indicating a reduction in environmental contamination as the implemented control measures limit active infection and parasite egg shedding. In contrast, the susceptible snail population increases steadily over the simulation period, while the exposed and latent snail populations exhibit an initial rise followed by a gradual decline to negligible levels. Overall, these numerical results suggest that the integrated intervention strategies effectively reduce environmental transmission and suppress infection among the intermediate snail hosts. This finding is consistent with Yuan-Han (2024), who demonstrated through a multi-group transmission model that sustained and integrated control measures can substantially reduce the long-term transmission of parasitic diseases.

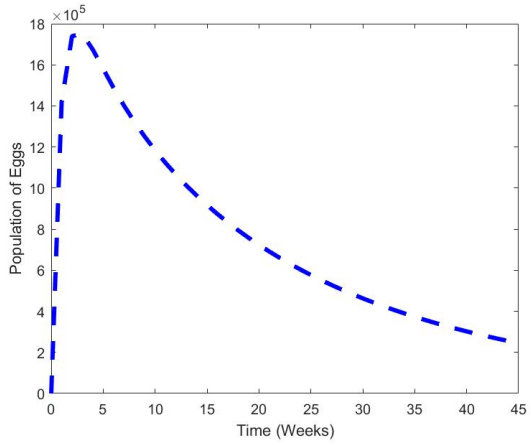

(i)Profile of $G(t)$

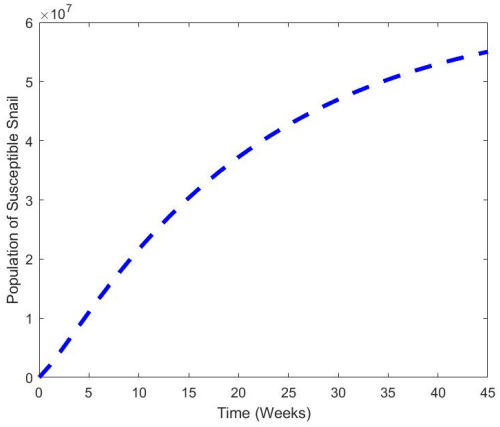

(j)Profile of $S_s(t)$

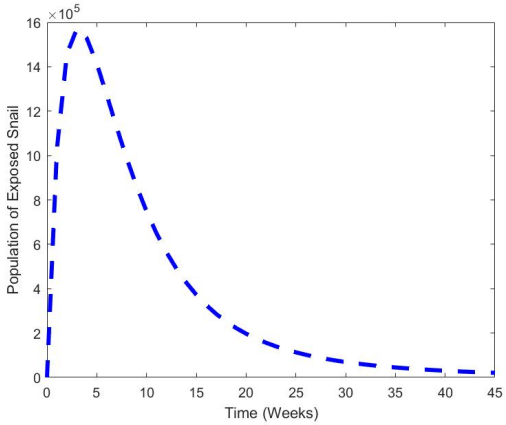

(k)Profile of $E_s(t)$

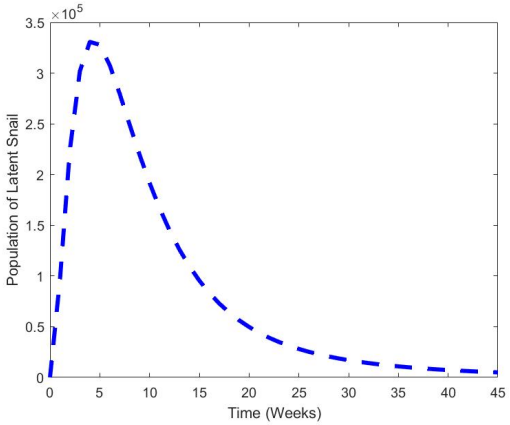

(l)Profile of $L_s(t)$

Figure 3: Dynamics of G, S_s,E_s and L_s population against time (week).

4.4 Behavior of I_s, D_s,C and S_c plotted against time (week).

Figures 4(m–p) present the 45-week temporal dynamics of the infected snail population (I_s), dead/incapacitated snail population (D_s), cercariae population (C), and susceptible crayfish population (S_c). The infected snail population initially rises to approximately 2.1×10^6 before gradually declining, while the dead/incapacitated snail population increases more slowly, reflecting the delayed effects of infection. The cercariae population reaches an early peak of about 1,050 before rapidly decreasing to near zero, indicating a substantial reduction in cercarial production and persistence in the aquatic environment. In contrast, the susceptible crayfish population declines sharply during the first 10–12 weeks, corresponding to the period of high cercarial abundance. Overall, these patterns suggest that the implemented control measures reduce infection among snail hosts and subsequently limit cercarial transmission to crayfish, thereby disrupting the aquatic transmission cycle of *Paragonimus*. This finding is consistent with Huang (2020), who demonstrated that sustained and targeted interventions can substantially reduce infection levels in trematode transmission systems and emphasized the importance of controlling intermediate hosts to limit continued parasite transmission.

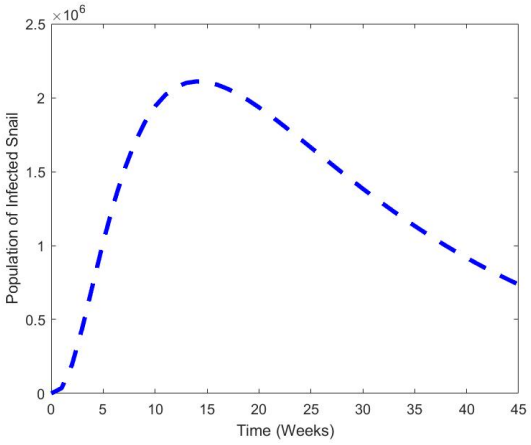

(m)Profile of $I_s(t)$

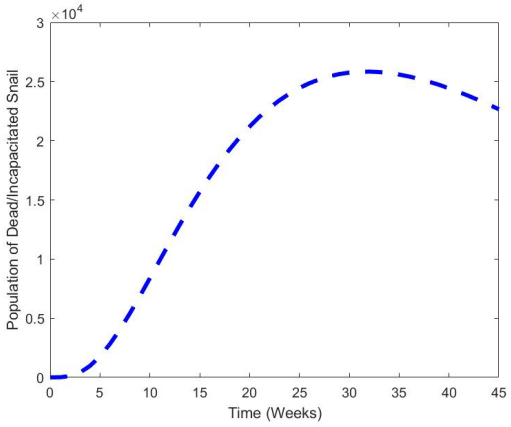

(n)Profile of $D_s(t)$

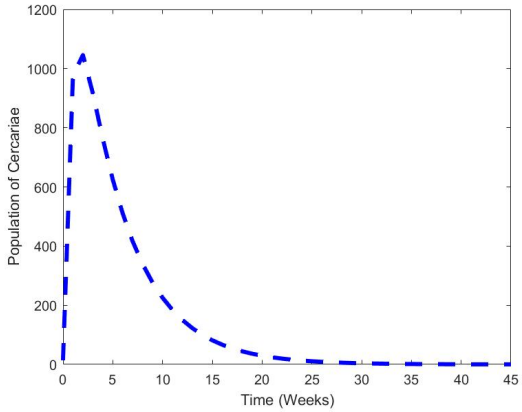

(o)Profile of $C(t)$

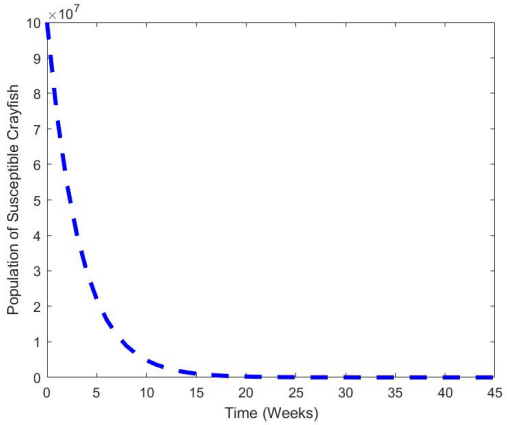

(p)Profile of $S_c(t)$

Figure 4: Dynamics of I_s, D_s,C and S_c population against time (week).

4.5 Behavior of E_c, L_c,I_c and D_c plotted against time (week).

The dynamic trajectories of exposed (E_c), latent (L_c), infected (I_c), and dead or incapacitated (D_c) crayfish populations over the 45-week simulation timeline are depicted in Figures 5 (q–t). The exposed and active infection classes exhibit swift early declines toward near-elimination, with the infected compartment dropping to approximately 3.304×10^{-6} by week 45. The latent population displays a transient initial spike, peaking at roughly 5×10^4 individuals within the first two weeks before rapidly vanishing. Similarly, the dead/incapacitated crayfish class reaches a maximum of approximately 2.2×10^4 around week 3 before tapering off. Collectively, these simulation profiles confirm a systematic clearance of infection within the crustacean reservoir and eventual convergence toward the disease-free equilibrium, demonstrating that the control framework successfully halts intermediate transmission. These findings align with those of Huang (2020), who demonstrated that targeted control interventions significantly suppress transmission intensity and parasite burdens within trematode host systems.

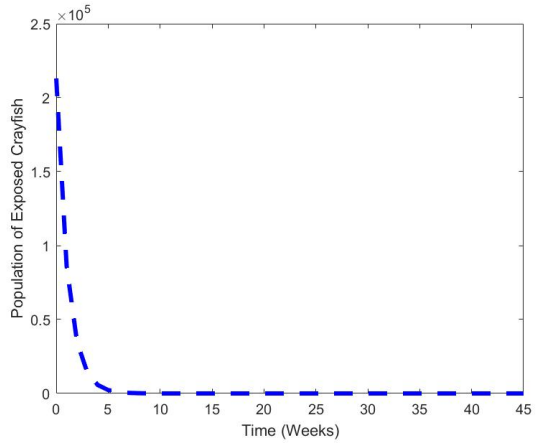

(q)Profile of $E_c(t)$

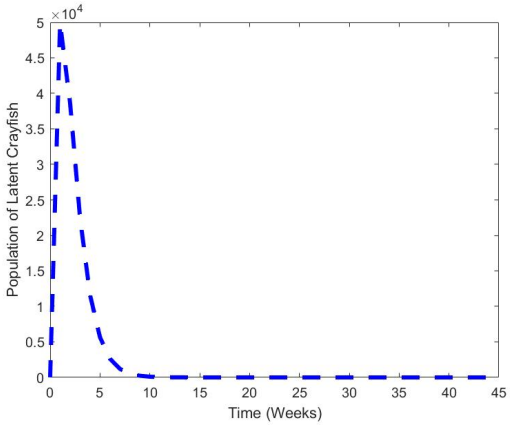

(r)Profile of $L_c(t)$

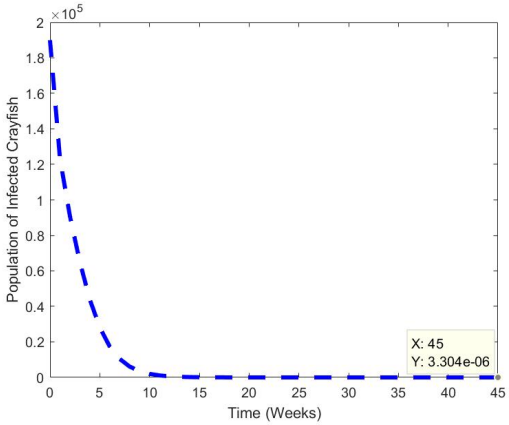

(s)Profile of $I_c(t)$

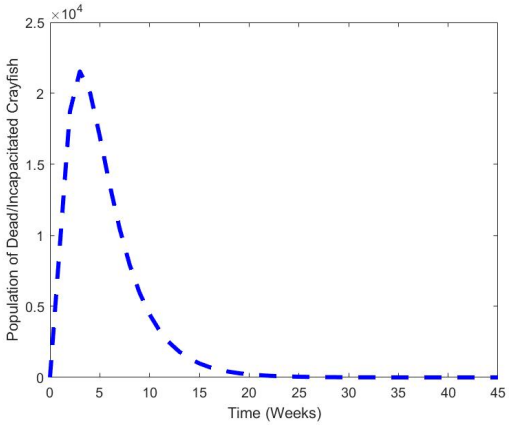

(t)Profile of $D_c(t)$

Figure 5: Dynamics of E_c, L_c,I_c and D_c population against time (week).

5 Conclusion

This study investigates the threshold dynamics and stability analysis of a mathematical model for *Paragonimiasis* dynamics, supported by numerical simulations. The basic reproduction number, R_0, was derived using the next-generation matrix approach to establish the conditions governing disease persistence or elimination. Stability analysis, based on the Routh–Hurwitz criterion and the Castillo–Chavez framework, demonstrated that the disease-free equilibrium is globally asymptotically stable when $R_0 < 1$. Sensitivity analysis further identified the key parameters that significantly influence R_0. In addition, numerical simulations illustrated the temporal behaviour of the model populations and showed that the combined application of appropriate intervention measures can certainly reduce disease transmission and accelerate its elimination. This findings provide useful biomathematical insights for developing effective public health strategies for the control and eventual elimination of *Paragonimiasis* in endemic society.

Availability of data and material

Not Applicable.

Competing Interest

No competing interest is hereby declared by the authors.

Funding

The research received no external funding.

Authors' contributions

The development of the model was done by Abdulfatai, Atte Momoh. Model analysis, discussion of results and typesetting were implemented by James John Yakoko. All authors approved the final manuscript.

Acknowledgments

The authors acknowledged the facilities provided by Modibbo Adama University, Yola, Nigeria and Tertiary Education Trust Fund.

Authors' information

[1] *Department of Mathematics,College of Education, Zing Taraba State, Nigeria .*

References

Castillo-Chavez, C., Feng, Z., Huang, W. (2002). On the Computation of R_0 and its Role on Global Stability. *Institute for mathematics and its applications*,125:229.

Chen, M. X., et al. (2011). Sensitive and Rapid Detection of Paragonimus westermani Infection in Humans and Animals by Loop-Mediated Isothermal Amplification (LAMP). *Parasitology Research*, 108, 1193–1198.

Diekmann, O., Heesterbeek, J. A. P., & Roberts, M. G. (2010). The Construction of Next-Generation Matrices for Compartmental Epidemic Models. *Journal of The Royal Society Interface*, 7(47), 873–885.

Dye, C. (1996). The logic of visceral leishmaniasis control. *The American journal of tropical medicine and hygiene*, 55(2), 125–130.

Edward, S. (2025). Caputo approach to transmission dynamics of paragonimiasis in humans, snails, and crustaceans. *Partial Differential Equations in Applied Mathematics*. 16.

Enwereji, E. E. and Eke, R. A. (2010). Re-Emergence of Paragonimiasis in Nigeria: A Case Report and Future Challenges. *TAF Preventive Medicine Bulletin*, Ankara, Turkey.

Huang, X. H., Qian, M. B., Zhu, G. H., Fang, Y. Y., Hao, Y. T., and Lai, Y. S. (2020). Assessment of control strategies against *Clonorchis sinensis* infection based on a multi-group dynamic transmission model. *PLoS Neglected Tropical Diseases*, 14(3), e0008152. doi:10.1371/journal.pntd.0008152.

Ibanga, E. S., Arene, F. O. I. and Asor, J. E. (2003). Association of Pulmonary

Paragonimiasis with Active Pulmonary Tuberculosis in Rural Yakurr Community in Cross River Basin, Nigeria. *Mary Slessor Journal of Medicine*, 3(1):19–23.

Iboh, C. I. (2018). Investigation of Crab-Eating Influence on Paragonimiasis Infection in Six Communities of Abayong from Cross River State Nigeria. *South Asian Journal of Parasitology*, 1(1):1–9. https://doi.org/10.9734/SAJP/2018/41742

Islam, S., Kenah, E., Bhuiyan, M. A. A., Rahman, K. M., Goodhew, B., Ghalib, C. M., & others (2013). Clinical and immunological aspects of post–kala-azar dermal leishmaniasis in bangladesh. *The American journal of tropical medicine and hygiene*, 89(2), 345.

Lili, L. N., Britton, N. F., and Feil, E. J. (2007). The Persistence of Parasitic Plasmids. *Genetics*, 177:399–405.

Menner, M. (2024). Translation of Nagumo's foundational work on barrier functions: On the location of integral curves of ordinary differential equations. *arXiv preprint arXiv:2406.18614*.

Nawa, Y. (2000). Re-emergence of Paragonimiasis. *Internal Medicine*, 39(5), 353–354.

Rahman, K. M., Islam, S., Rahman, M. W., Kenah, E., Galive, C. M., Zahid, M., & others (2010). Increasing incidence of post-kala-azar dermal leishmaniasis in a population-based study in bangladesh. *Clinical Infectious Diseases*, 50(1), 73–76.

Stauch, A., Sarkar, R. R., Picado, A., Ostyn, B., Sundar, S., Rijal, S., & Duerr, H.-P. (2011). Visceral leishmaniasis in the indian subcontinent: modelling epidemiology and control. *PLoS neglected tropical diseases*, 5(11), e1405.

World Health Organization (2022). Neglected tropical diseases: Paragonimiasis. Retrieved from https://www.who.int/news-room/questions-and-answers/item/neglected-tropical-diseases-paragonimiasis

Yakoko, J. J. et al. (2024). Mathematical Model for the Dynamics of Paragonimiasis Disease in Human, Snail, and Crustacean Populations. *International Journal of Development Mathematics*, 1(1), 90–110.

Yan, S. S. and Gilbert, J. M. (2004). Antimicrobial Drug Delivery in Food Animals and Microbial Food Safety Concerns. *Advanced Drug Delivery Reviews*, 56, 1497–1521.

Yuan, R. et al. (2018). Modeling the Transmission Dynamics of Clonorchiasis in Foshan, China. *Scientific Reports*, 8(1), 1–9. https://doi.org/10.1038/s41598-018-33431-w

Yuan-Han, H. (2024). Optimal Control Problems in Complex System: The Combination of Mathematical Modeling and Optimization Strategies. *International Journal of Education and Humanities in Academic*, 15(1).

Zhang, Q. et al. (2006). Fitness of Antimicrobial-Resistant Campylobacter and Salmonella. *Microbes and Infection*, 8.